CHEMICAL THERMODYNAMICS
AND THERMOCHEMISTRY

Synthesis, Crystal Structure, and the Optical and Thermodynamic Properties of $PrAlGe_2O_7$

L. A. Irtyugo[a,*], **L. T. Denisova**[a], **M. S. Molokeev**[a,b], **V. M. Denisov**[a],
A. S. Aleksandrovsky[a,b], **V. V. Beletskii**[a], and **E. Yu. Sivkova**[a]

[a]*Siberian Federal University, Krasnoyarsk, 660041 Russia*
[b] *Kirensky Institute of Physics, Krasnoyarsk Scientific Center, Siberian Branch,
Russian Academy of Sciences, Krasnoyarsk, 660036 Russia*
*e-mail: lirtugo@sfu-kras.ru

Abstract—Germanate $PrAlGe_2O_7$ is obtained from initial oxides Pr_2O_3, Al_2O_3, and GeO_2 via solid-phase synthesis. The crystal structure of the investigated germanate is determined via X-ray diffraction. The luminescence spectra are been determined at room temperature. The effect temperature has on the heat capacity is determined via differential scanning calorimetry. The thermodynamic properties of the complex oxide compound are calculated using the experimental data on $C_p = f(T)$ in the temperature range of 350−1000 K.

INTRODUCTION

There has recently been a steady rise in interest in germanium-based oxide materials with the general formula $RMGe_2O_7$ (R = rare-earth element (REE); M = Al, Ga, In, Fe) [1−7]. It should be noted that the compounds most studied also contain iron [4, 5, 8−12], and we have data on their structure and magnetic properties. Only fragmentary data on unit cell parameters and optical properties are available for other $RMGe_2O_7$ compounds [1, 2, 5, 7]. The thermophysical properties of this type of compounds at high temperatures have been investigated only for $SmFeGe_2O_7$ [12] and $SmGaGe_2O_7$ [7]. These materials include $PrAlGe_2O_7$, for which only unit cell parameters are known [2]. Dielectrics that contain Pr are objects of great interest from the viewpoint of their optical properties (see, e.g., [13]).

The aim of this work was to synthesize, determine the crystal structure, and study the luminescence and thermodynamic properties of $PrAlGe_2O_7$ germanate.

EXPERIMENTAL

Germanate $PrAlGe_2O_7$ was obtained from initial oxides Pr_2O_3, Al_2O_3, and GeO_2 via solid-phase synthesis. Pr_2O_3 was obtained from Pr_6O_{11} via reduction with hydrogen according to the procedure described in [14]. A stoichiometric mixture of the initial oxides was thoroughly ground in an agate mortar and pressed into pellets, which were then sequentially calcined in air at temperatures of 1273 (40 h), 1373 (100 h), and 1473 K (60 h). To ensure completion of the solid-state reaction, the pellets were ground every 20 h and the resulting powders were pressed into pellets again. The synthesis time and the amount of excess GeO_2 (the relatively high temperatures of germanate synthesis result in partial evaporation of the GeO_2 [15]) were optimized using experimental data. The phase composition of the obtained samples was monitored via X-ray structural analysis.

The X-ray powder diffraction pattern of $PrAlGe_2O_7$ was obtained on a Bruker D8 ADVANCE diffractometer using a VANTEC linear detector (CuK_α radiation) at room temperature. During each experiment, a primary beam slit of 0.6 mm was used in angular range $2\theta = 11°−120°$. The 2θ angle scanning step was $0.016°$ and the exposure time was 2 s per step. The luminescence spectra were measured on a Horiba-Jobin-Yvon T6400 spectrometer at room temperature. The heat capacity of $SmGaGe_2O_7$ was measured on a NETZSCH STA 449 C Jupiter unit (Germany). The experimental procedure is similar to the one described in [16]. At least three independent heat capacity measurements were made. The uncertainty in our heat capacity measurements at temperatures above 373 K

Table 1. Crystal structure parameters of $PrAlGe_2O_7$ (sp. gr. $P21/c$)

Parameter	Value
a, Å	7.2292(1)
b, Å	6.5329(1)
c, Å	12.7470(2)
β, deg	117.4096(9)
V, Å^3	534.41(1)
2θ angle range, deg	11−120
R_{wp}, %	5.09
R_p, %	3.65
R_B, %	1.13
χ^2	1.91

Table 2. Atomic coordinates and isotropic heat parameters B_{iso} (Å^2) of the $PrAlGe_2O_7$ structure

| Atom	x	y	z	B_{iso}
Pr	0.7618(2)	0.1477(3)	0.02502(12)	0.58(9)
Al	0.7894(11)	0.3970(12)	0.2682(5)	0.45(17)
Ge1	0.7908(4)	0.6561(5)	0.0497(2)	0.71(11)
Ge2	0.3022(4)	0.4077(4)	0.2190(3)	0.40(10)
O1	0.587(2)	0.822(2)	0.0238(10)	0.50(15)
O2	0.7652(18)	0.126(2)	0.2173(10)	0.50(15)
O3	0.5703(19)	0.388(2)	0.2963(11)	0.50(15)
O4	0.006(2)	0.331(2)	0.4178(10)	0.50(15)
O5	0.744(2)	0.007(2)	0.4251(12)	0.50(15)
O6	0.8019(19)	0.4456(19)	0.1392(12)	0.50(15)
O7	0.166(2)	0.184(2)	0.1902(12)	0.50(15)

was within 2%. The experimental data were analyzed using the Netzsch Proteus Thermal Analysis program package and licensed Systat Sigma Plot 12 graphing software (Systat Software Inc., United States).

RESULTS AND DISCUSSION

With the exception of the impurity peaks, almost all reflections are assigned to a monoclinic cell with parameters close to that of $SmFeGe_2O_7$ [17]. This structure was therefore taken as the initial model for Rietveld refinement using the TOPAS 4.2 program [18]. For the conversion, the Sm site was replaced with a Pr ion, and Fe was replaced with Al. The results from refinement are given in Table 1 and in

Fig. 1. The atomic coordinates and main bond lengths for $PrAlGe_2O_7$ are given in Tables 2 and 3, respectively. The structure of the germanate is shown in Fig. 2. A comparison of the $PrAlGe_2O_7$ unit cell parameters we obtained (Table 1) and the data in [2] (a = 7.23(1) Å, b = 6.53(1) Å, c = 12.75(1) Å, β = 1l7.5(2)°, d = 5.29 g/cm^3) shows their good agreement.

The luminescence spectrum of $PrAlGe_2O_7$, recorded upon excitation by an InGaN laser at 450 nm, is shown in Fig. 3. The wavelength of excitation falls into resonance with $^3H_4$–$^3P_2$ transition with subsequent relaxation to states $^3P_0$ and $^3P_1$. The luminescence spectrum is formed mainly by contributions from the transitions from these states of the Pr^{3+} ion.
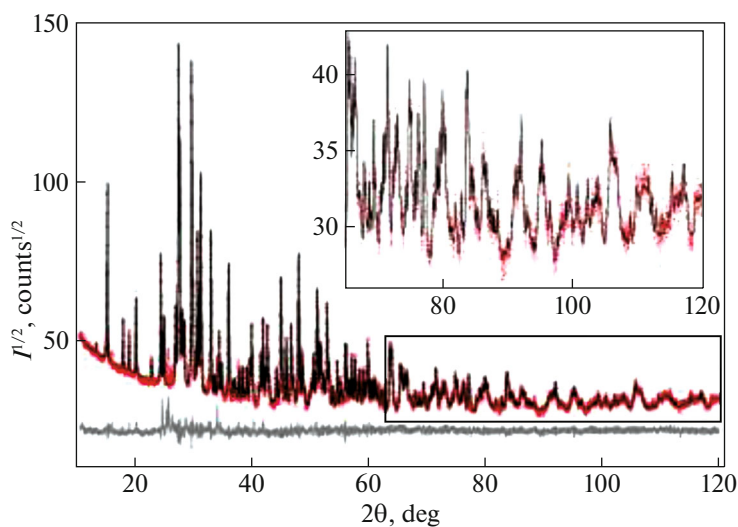
Fig. 1. Rietveld refinement of X-ray diffraction pattern for $PrAlGe_2O_7$.

Table 3. Main bond lengths (Å) in the PrAlGe$_2$O$_7$ structure

Bond	Bond length	Bond	Bond length
Pr–O1[i]	2.472(13)	Al–O4[vi]	1.876(13)
Pr–O1[ii]	2.309(10)	Al–O6	1.718(14)
Pr–O2	2.444(11)	Al–O7[vii]	1.937(15)
Pr–O3[iii]	2.599(13)	Ge1–O1	1.735(12)
Pr–O4[iv]	2.552(12)	Ge1–O4[vii]	1.755(11)
Pr–O4[v]	2.686(9)	Ge1–O5[iii]	1.756(13)
Pr–O5[iii]	2.647(13)	Ge1–O6	1.765(13)
Pr–O6	2.367(13)	Ge2–O2[vii]	1.814(13)
Pr–O7[vi]	2.713(11)	Ge2–O3	1.728(9)
Al–O2	1.868(16)	Ge2–O5[vii]	1.797(13)
Al–O3	1.778(9)	Ge2–O7	1.703(12)

Elements of symmetry: (i) x, $y − 1$, z; (ii) $−x + 1$, $−y + 1$, $−z$; (iii) x, $−y + 1/2$, $z − 1/2$; (iv) $−x + 1$, $y − 1/2$, $−z + 1/2$; (v) $x + 1$, $−y + 1/2$, $z − 1/2$; (vi) $x + 1$, y, z; and (vii) $−x + 1$, $y + 1/2$, $−z + 1/2$.

The fading wing in the short-wavelength part of the spectrum is scattered radiation from the source of excitation. The predominance of the exciting radiation confirms that the observed luminescence of the highly concentrated PrAlGe$_2$O$_7$ crystal is fairly weak, which must be attributed to the radiativeless transfer of energy between Pr ions and thus to concentration quenching of the luminescence. The main bands of Pr^{3+} luminescence identified in the spectrum correspond to the $^3P_0$–$^3H_4$, $^3P_1$–$^3H_5$, $^3P_0$–$^3H_5$, $^1D_2$–$^3H_4$, $^3P_0$–$^3H_4$, $^3P_0$–$^3H_6$, $^3P_0$–$^3F_2$, $^3P_0$–$^3F_3$, and $^3P_0$–$^3F_4$ transitions. The presented spectrum shows convincingly that in addition to concentration quenching, there is an additional effect from the high concentra-

tion of Pr: the reabsorption of emitted luminescence. This effect is observed if the characteristic length of flight of emitted photons in the material is comparable to or less than the one at the wavelength of excitation. Naturally, this effect is observed only at luminescent transitions terminating at the ground state ($^3H_4$). The band corresponding to $^3P_0$–$^3H_4$ transition is considerably diminished, due to reabsorption in the PrAlGe$_2$O$_7$. The same effect can be seen for the $^1D_2$–$^3H_4$ transition, which is notably reduced in comparison to the neighboring $^3P_0$–$^3H_6$ band.

We should note the relatively broad and structureless spectral feature peaking at 700 nm, which cannot be ascribed to any transition of the Pr ion forbidden by parity. It is presumably explained by the presence of such minor crystal structure defects as anion vacancies. The optical transitions of these defects are allowed by parity and typically produce broad spectral features in luminescence and absorption. It follows, however, that the content of these defects is much lower than that of Pr ions.

Figure 4 presents the temperature dependence of the heat capacity of PrAlGe$_2$O$_7$. We can see that dependence $C_p = f(T)$ contains no extrema. We may therefore assume that PrAlGe$_2$O$_7$ has no polymorphic transformations in the considered range of temperatures. The data is described by the classical Maier–Kelley equation [19]

$$C_p = a + bT - cT^{-2}, \qquad (1)$$

which has the following form for PrAlGe$_2$O$_7$:

$$C_p = (234.40 \pm 0.72) + (74.79 \pm 0.80) \times 10^{-3}T \\ - (42.67 \pm 0.78) \times 10^5 T^{-2}. \qquad (2)$$
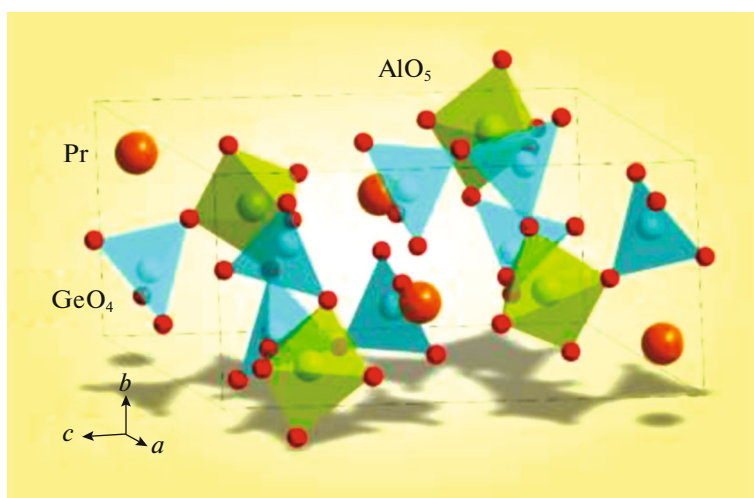
Fig. 2. Crystal structure of PrAlGe$_2$O$_7$.
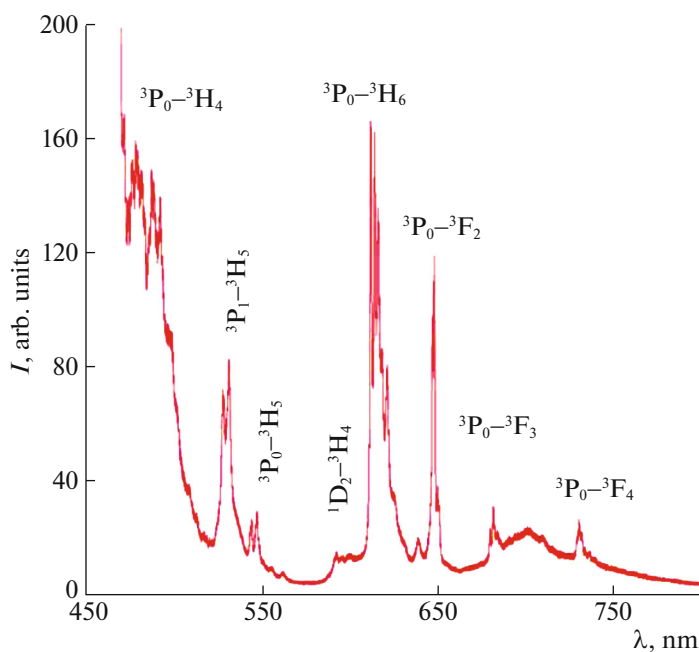
Fig. 3. Luminescence spectrum of $PrAlGe_2O_7$.

The coefficient of correlation in Eq. (2) is 0.9996, and the maximum deviation of the experimental points form the smoothing curve is 0.66%.

Using Eq. (2) and familiar thermodynamic relations, we determined the thermodynamic functions of the germanate $PrAlGe_2O_7$. The results are presented in Table 4.

There are no literature data on the specific heat of $PrAlGe_2O_7$, so we were unable to compare our data and results obtained by other authors. At the same time, this can be done with calculated C_p values using different model concepts: Neumann−Kopp (NK) [20−22] and the incremental Kumok approach (IMK) [23]. These data are presented in Table 5. We can see that the incremental Kumok approach gives the best

Table 4. Smoothed values of the molar heat capacity and calculated values of enthalpy $H^0(T) - H^0(350 \text{ K})$, entropy $S^0(T) - S^0(350 \text{ K})$, and normalized Gibbs energy $(\Delta G/T)$ for $PrAlGe_2O_7$

T, K	C_p, J mol^{-1} K^{-1}	$H^0(T) - H^0(350 \text{ K})$, kJ mol^{-1}	$S^0(T) - S^0(350 \text{ K})$, J mol^{-1} K^{-1}	$-\Delta G/T$*, J mol^{-1} K^{-1}
350	225.8	—	—	—
400	237.7	11.60	30.96	1.96
450	247.0	23.72	59.51	6.79
500	254.7	36.27	85.95	13.40
550	261.5	49.18	110.5	21.13
600	267.4	62.41	133.6	29.55
650	272.9	75.92	155.2	38.39
700	278.1	89.70	175.6	47.47
750	282.9	103.7	195.0	56.66
800	287.6	118.0	213.4	65.88
850	292.1	132.5	230.9	75.08
900	296.5	147.2	247.8	84.21
950	300.7	162.1	263.9	93.25
1000	305.0	177.3	279.4	102.2

* $-\Delta G/T = [H^0(T) - H^0(350 \text{ K})]/T - [S^0(T) - S^0(350 \text{ K})]$.
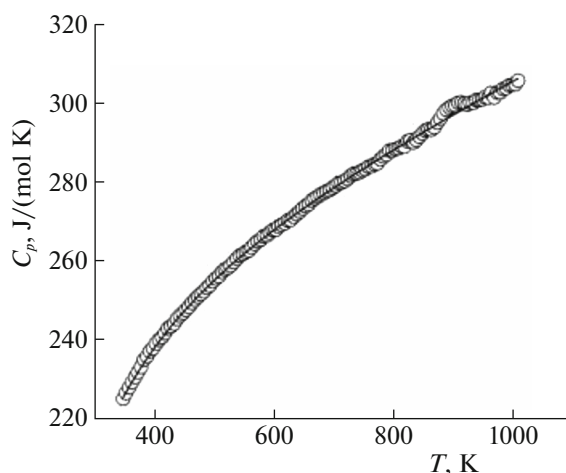
Fig. 4. Temperature dependences of the molar heat capacity for $PrAlGe_2O_7$. The white dots are experimental data; the line is the best fit curve.

Table 5. Comparison of our experimental C_p(298 K) data (J mol^{-1} K^{-1}) and calculation results obtained using different model equations

Compound	$C_{p,298}$	NK	Δ, %	IMK	Δ, %
$PrAlGe_2O_7$	208.7	201.7	−3.4	212.0	+1.6

agreement with the experiment. The C_p values for binary oxides Pr_2O_3, Al_2O_3, and GeO_2 required for NK calculations were taken from [20].

CONCLUSIONS

Alumogermanate $PrAlGe_2O_7$ was synthesized by annealing a stoichiometric mixture of Pr_2O_3, Al_2O_3, and GeO_2 in air at 1273−1473 K. Its crystal structure was determined. Its luminescent properties were investigated, and its thermodynamic functions in the range of 350−1000 K were determined.

CONFLICT OF INTEREST

The authors declare they have no conflicts of interest.

REFERENCES

1. O. Jarchow, K.-H. Klaska, and H. Schenk-Strauß, Z. Kristallogr. **172**, 159 (1985).

2. A. A. Kaminskii, B. V. Mill, A. V. Butashin, et al., Phys. Status Solidi A **103**, 575 (1987).

3. G. Lozano, C. Cascales, C. Zaldo, et al., J. Alloys Compd. **303**−**304**, 349 (2000).

4. E. J. Baran, C. Cascales, and R. C. Mercader, Spectrochim. Acta, Part A **56**, 1277 (2000).

5. E. A. Juarez-Arellano, J. Campa-Molina, S. Ulloa-Godinez, et al., Mater. Res. Soc. Symp. Proc. **848**, FF6.15.1 (2005).

6. A. A. Kaminskii, H. Rhee, O. Lux, et al., Laser Phys. Lett. **10**, 075803 (2013).

7. L. T. Denisova, M. S. Molokeev, L. A. Irtyugo, V. V. Beletskii, N. V. Belousova and V. M. Denisov, Phys. Solid State **62**, 384 (2020).
https://doi.org/10.1134/S1063783420020109

8. B. V. Mill', Z. A. Kazei, S. I. Reiman, et al., Vestn. Mosk. Univ., Ser. 3: Fiz. Astron. **28** (4), 95 (1987).

9. L. Bucio, C. Cascales, and J. A. Alonso, J. Phys.: Condens. Matter **8**, 2641 (1996).

10. C. Cascales, E. Gutiérrez Puebla, S. Klimin, et al., Chem. Mater. **11**, 2520 (1999).

11. C. Cascales, M. T. Fernéz-Diaz, and M. A. Monge, et al., Chem. Mater. **14**, 1995 (2002).

12. L. T. Denisova, A. D. Izotov, Yu. F. Kargin, and L. A. Irtygo, Dokl. Phys. Chem. **487**, 109 (2019).
https://doi.org/10.1134/S0012501619080050

13. W. Dong, Y. Sun, Q. Yao, et al., J. Lumin. **225**, 117288 (2020).
https://doi.org/10.1016/j.jlumin.2020.117288

14. L. T. Denisova, Yu. F. Kargin, L. G. Chumilina, V. M. Denisov, and S. D. Kirik, Inorg. Mater. **50**, 482 (2014).
https://doi.org/10.1134/S0020168514050045

15. U. W. Becker and J. Felsche, J. Less-Common Met. **128**, 269 (1987).

16. L. T. Denisova, L. A. Irtyugo, N. V. Belousova, V. V. Beletskii, and V. M. Denisov, Russ. J. Phys. Chem. A **93**, 598 (2019).
https://doi.org/10.1134/S004445371903004X

17. T. V. Drokina, G. A. Petrakovskii, D. A. Velikanov, and M. S. Molokeev, Phys. Solid State **56**, 1131 (2014).

18. *Bruker AXS TOPAS V4: General Profile and Structure Analysis Software for Powder Diffraction Data, User's Manual* (Bruker AXS, Karlsruhe, Germany, 2008).

19. C. G. Maier and K. K. Kelley, J. Am. Chem. Soc. **54**, 3242 (1932).

20. J. Leitner, P. Chuchvaler, D. Sedmidubský, et al., Thermochim. Acta **395**, 27 (2003).

21. G. K. Moiseev, N. A. Vatolin, L. A. Marshuk, and N. I. Il'inykh, *Temperature Dependences of the Reduced Gibbs Energy of Some Inorganic Substances* (UrO RAN, Yekaterinburg, 1997) [in Russian].

22. A. G. Morachevskii, I. G. Sladkov, and E. G. Firsova, *Thermodynamic Calculations in Chemistry and Metallurgy* (Lan', St. Petersburg, 2018) [in Russian].

23. V. N. Kumok, *Direct and Inverse Problems of Chemical Thermodynamics* (Nauka, Sib. Otd., Novosibirsk, 1987), p. 108 [in Russian].